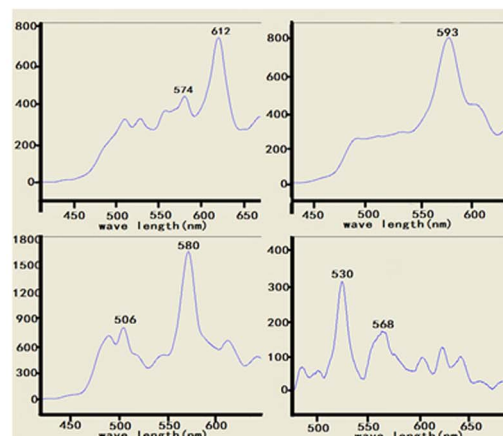
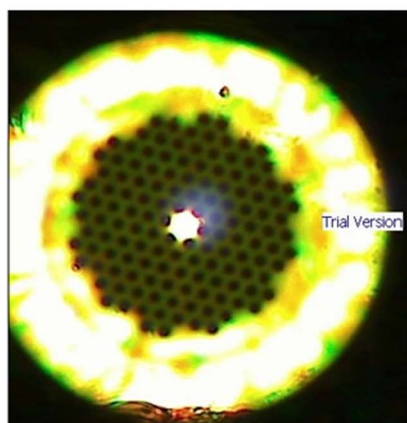
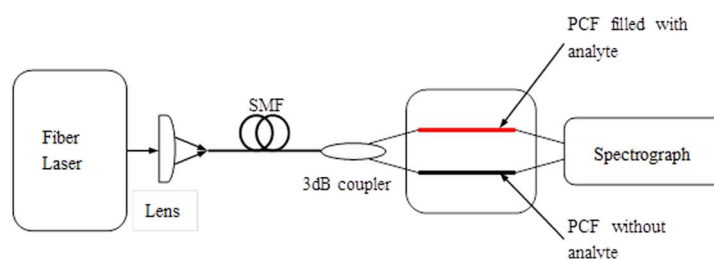


Temperature Sensing Using Photonic Crystal Fiber Filled With Silver Nanowires and Liquid

Volume 6, Number 3, June 2014

Y. Lu
M. T. Wang
C. J. Hao
Z. Q. Zhao
J. Q. Yao



DOI: 10.1109/JPHOT.2014.2319086
1943-0655 © 2014 IEEE

Temperature Sensing Using Photonic Crystal Fiber Filled With Silver Nanowires and Liquid

Y. Lu, M. T. Wang, C. J. Hao, Z. Q. Zhao, and J. Q. Yao

Institute of Laser and Opto-electronics, College of Precision Instrument and Opto-electronics Engineering, Key Laboratory of Opto-electronics Information Technology (Ministry of Education), Tianjin University, Tianjin 300072, China

DOI: 10.1109/JPHOT.2014.2319086

1943-0655 © 2014 IEEE. Translations and content mining are permitted for academic research only. Personal use is also permitted, but republication/redistribution requires IEEE permission. See http://www.ieee.org/publications_standards/publications/rights/index.html for more information.

Manuscript received April 8, 2014; accepted April 11, 2014. Date of publication April 22, 2014; date of current version May 5, 2014. This work was supported in part by the National Basic Research Program of China (973 Program) under Grant 2010CB327801 and in part by the National Natural Science Foundation of China under Grant 10874128. Corresponding author: Y. Lu (e-mail: luying@tju.edu.cn).

Abstract: A temperature sensor based on photonic crystal fiber (PCF) surface plasmon resonance (SPR) is proposed in this paper. We use the dual function of the PCF filled with different concentrations of analyte and silver nanowires to realize temperature sensing. The proposed sensor has been analyzed through numerical simulations and demonstrated by experiments. The results of the simulations and experiments show that a blue shift will be obtained with the temperature increase, and different concentrations will change the resonance wavelength and confinement loss. Temperature sensitivity is as high as 2.7 nm/°C with the experiment, which can provide a reference for the implementation and application of a PCF-based SPR temperature sensor or other PCF-based SPR sensing.

Index Terms: Photonic crystal fiber, temperature sensor, silver nanowires, surface plasmon resonance.

1. Introduction

In recent years, photonic crystal fibers (PCFs) have been widely investigated for their special structure and unique properties. And there are so many investigators that interest in designing PCFs for use as advanced sensors by infiltrating the air holes with polymer [1], oil [2], gas [3], liquid [4], or liquid crystal [5]. Sensors based on PCFs with unique properties and design flexibility, are expected to overcome the difficulties and gradually becoming a new research focus [6]. PCF-based surface plasmon resonance (SPR) sensors specially gather continuous research interests in medical diagnostics, environmental control, drug control and food safety control [7], which is due to the characteristics of low cost fabrication, simple measurement system, and capability of remote sensing [8]–[10]. PCF-based SPR sensing can be realized when the phase matching condition is met between the exciting light and the surface plasmons [11]–[14]. In the past years, PCF-based SPR sensors for using in refractive index sensing of aqueous environment have promoted the development of the fiber optic sensors. Zhou *et al.* presented a PCF-based sensor, and the numerical simulation demonstrates that the measurement range of analyte index from 1.25 to 2.75 can be achieved [15]. The hybrid mechanism surmounts the limitation of the detection range of high-index coating sensors. In 2012, Shuai *et al.* reported a multi-core holey fiber based plasmonic

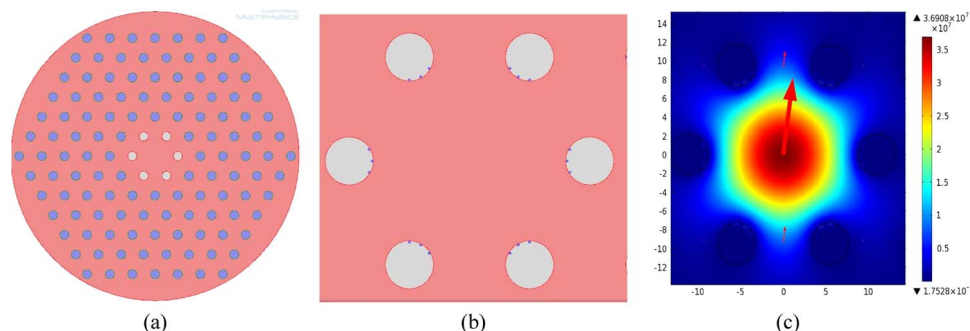


Fig. 1. (a) Cross section of the produced PCF-SPR temperature sensor. (b) Cross section of analyte channel filled with nanowires. (c) Electric field distribution of the fundamental mode.

sensor with a large detection range and high linearity, and they obtained an average sensitivity of 2929.39 nm/RIU in the sensing range 1.33-2.72, and 9231.27 nm/RIU in 2.73-1.53 through numerical simulation [4].

With the development of the sensors, and the propagation modes of PCF are highly temperature-dependent [5], [16], [17] PCF-base SPR sensing has involved in temperature sensors. These sensors can realize temperature sensing by adding some liquid with high thermo-optic coefficient into the air holes. In 2010, Yu *et al.* reported a new type of total internal reflection (TIR) PCF temperature sensor filled with ethanol, which is based on the strength of the modulation [18]. In 2012, Peng *et al.* had demonstrated a temperature sensor based on surface plasmon resonances supported by PCFs, and numerically calculated a temperature sensitivity of 720 pm/°C [19], and in 2013 they had proposed a temperature sensor using the bandgap-like effect [20]. However, the PCF-based SPR temperature sensors are based on the numerical simulation, the related report of the experiment is rare.

In this paper, we analyzed theoretically a temperature sensor based on SPR with large mode area (LMA)-8 PCF for an aqueous environment with different concentrations. We analyze the sensor through the finite element method (FEM), the relationship between the resonant wavelength and temperature has been numerically simulated, and resonant wavelength detection as well as intensity detection sensitivity has also been discussed. In order to demonstrate the feasibility of the temperature sensor, some related experiments with different concentrations and different temperatures have been carried out. The experimental results present that the resonance peaks have a blue shift when the temperature increases and the confinement loss will change. This work can realize the experiment of PCF-based temperature sensing based on SPR effect, which can provide reference for the implementation and application of PCF-based SPR temperature sensor or other PCF-based SPR sensing.

2. Theoretical Modeling

The schematic geometry of the PCF-based SPR temperature proposed in this paper is shown in Fig. 1(a), which is based on the LMA-8 PCF produced by NKT Photonics. The diameters of the core and cladding are approximately $d_c = 8 \mu\text{m}$ and $d = 125 \mu\text{m}$, respectively. The whole cladding is consisting of six layers air holes of hexagonal lattices. In this work, the full-vectorial FEM is used to calculate the effective indices of electromagnetic modes supported by the designed temperature sensor. In the numerically simulation, we take the air holes of the first layer as the liquid channels and some silver nanowires embedded in them. The cross-section of the channels with analyte and silver nanowires is shown in Fig. 1(b). The purpose of the design is to enhance the coupling between a core-guided mode and a plasmonic mode, and simultaneously to reduce the plasmonic to plasmonic mode coupling [19], [20].

The proposed PCF takes fused silica as the background material, which is a single-material optical fiber that can be obtained by the well developed stack-and-draw fabrication process [4]. The refractive index of fused silica optical fiber can be determined by Sellmeier equation and the relative

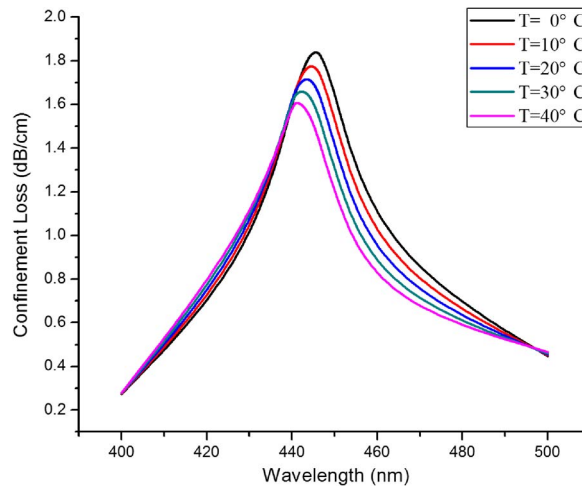


Fig. 2. Shift in resonant wavelength of the loss spectrum for a variation in temperatures of the proposed PCF-SPR sensor.

dielectric constant of silver is referred to the Handbook of Optics. According to the simulation, the effective refractive index of surface plasmons resonance mode can be obtained, which is dependent on the silver nanowires, the background fused silica, and the adjacent analyte. The electric field distribution calculated by the commercial software COMSOL with scattering boundary condition is presented in Fig. 1(c). It is obvious to note that according to the function of cladding air holes the formed fundamental modes are confined well within the core, and the arrows indicate the electric field direction.

To investigate the influence of temperature on the proposed PCF-based temperature sensor, different temperatures ($T = 0\text{ }^{\circ}\text{C}$, $10\text{ }^{\circ}\text{C}$, $20\text{ }^{\circ}\text{C}$, $30\text{ }^{\circ}\text{C}$, $40\text{ }^{\circ}\text{C}$) have been defined. The simulation results are presented in Fig. 2, which show that the phase-matching wavelength between the plasmonic mode and the core-guided mode changes, when refractive indices of the constituents of the proposed sensor vary with temperature. Therefore, the loss peak can be shifted when the RI of the silica, analyte, and the filled silver nanowires change with the temperature changing. From the Fig. 2, it can be obviously seen that there are a blue-shift and a change of the confinement loss when the temperature increases.

The quantitative description can be with the attenuation constant α of the fundamental mode, which can be evaluated by

$$\alpha = 2k_0 \text{Im}(n_{\text{eff}}) \quad (1)$$

where k_0 is the wave number ($k_0 = 2\pi/\lambda$), $\text{Im}(n_{\text{eff}})$ is imaginary part of the mode effective refractive index. Confinement loss is the light confinement ability within the core region. And the corresponding confinement loss of fiber expression is

$$\alpha_{\text{loss}} = 10 \lg e \cdot \alpha = 4.343\alpha. \quad (2)$$

When the phase matching is satisfied at a certain wavelength regime, the energy of a core-guided mode is transferred to plasmonic mode. And an increase in the loss will be observed at this wavelength regime.

To make a comprehensive understanding of the influence of filled analyte and nanowires, the filling analyte is defined with different concentrations of solution of silver nanowires (C_{Ag}) and ethanol (C_{eth}), which are 1 : 2, 1 : 3, 1 : 4, respectively. The filled liquid medium has a large thermo-optic coefficient, and the variations of dielectric constants for all components of wavelength have been taken into account. The simulation results of different concentrations filled in the channels are shown in Fig. 3, which exhibits that different concentrations have an effect on the confinement loss and the resonant wavelength. There is a blue-shift with the increase of the ratio of

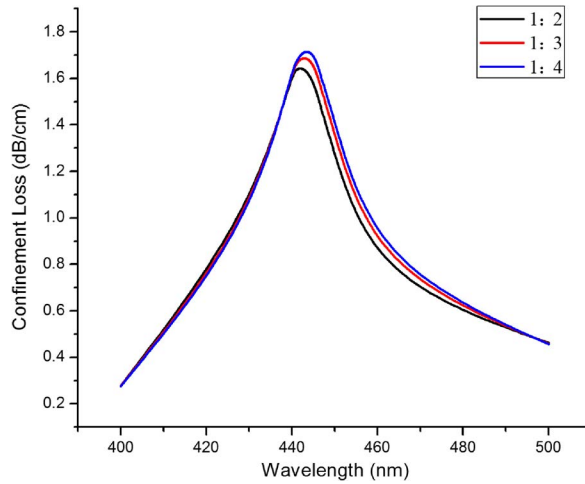


Fig. 3. Shift in resonant wavelength of the loss spectrum for a variation in different concentrations of solution with the same temperature of the proposed PCF-SPR sensor.

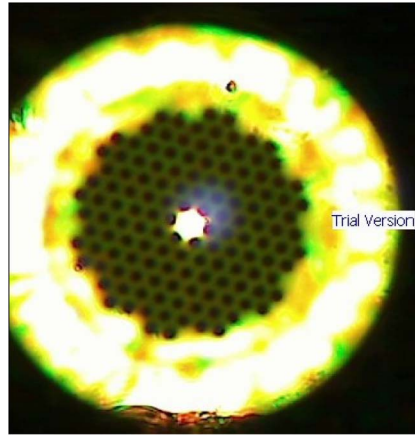


Fig. 4. Optical microscope images of cross-section of LMA-8.

ethanol, which can be explained by that the change of the refractive index of analyte will vary the resonant wavelength.

In a spectrum-based detection method, changes in the temperature are detected by measuring the shift of the loss peak λ_{peak} [21]. The sensitivity can be defined as

$$S_{\lambda} [\text{nm}/^{\circ}\text{C}] = \frac{d\lambda_{\text{peak}}(T)}{dT}. \quad (3)$$

According to the numerical simulation and discussion, it can be seen that the sensitivity is $200 \text{ pm}/^{\circ}\text{C}$ for $0\text{--}40^{\circ}\text{C}$ detection range. In addition, the confinement loss and sensing sensitivity are not only influenced by the changes of temperature, as are the mass-mixing ratio of the filling concentrations.

3. Experimental Setup and Analysis

To confirm the implementing corresponding to the theory modeling, the LMA-8 PCF with the same geometry is used in the experiment. The cross-section of the LMA-8 PCF is shown in Fig. 4. The analyte with silver nanowires are full-filled into the air holes by capillary force and air pressure. In

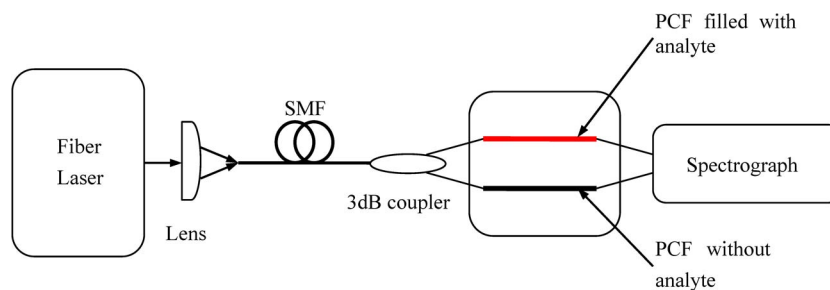


Fig. 5. Scheme of the experimental setup for PCF-based SPR temperature sensor.

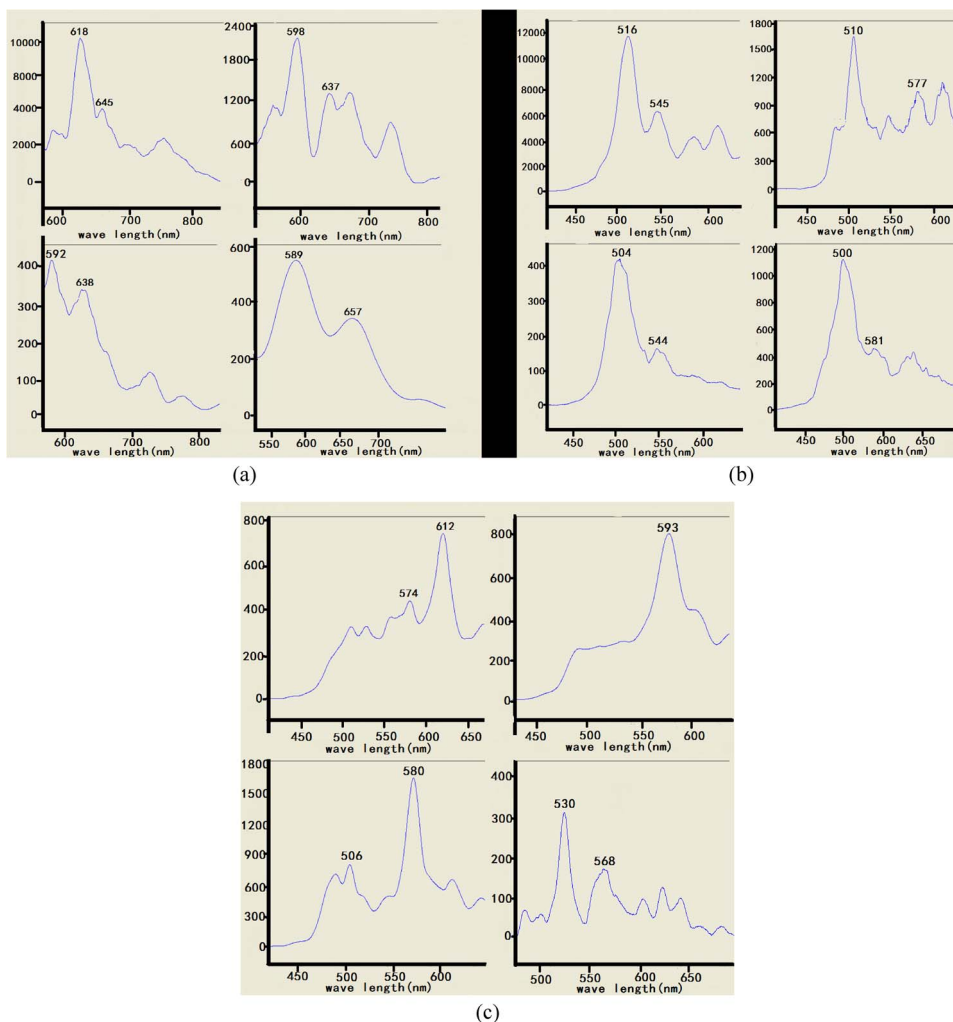


Fig. 6. Change in the resonant peaks from 10 °C to 40 °C as a function of wavelength with different ratios of the analyte. (a) 1 : 2 (b) 1 : 3 (c) 1 : 4.

addition, the refractive index of the filling is lower than the fused silica core to guarantee the total index-guiding mechanism and the corresponding reflection condition.

Taking the LMA-8 PCF filled with analyte and nanowires as the medium of transmission and sensing, a scheme of the experimental setup for the temperature-dependence measurement is designed to investigate the temperature sensing properties. The system is presented in Fig. 5. In

TABLE 1

Resonant peaks shift from 10 °C to 40 °C with different ratios of analyte

Resonance Ratio \ Temperature Peak	10	20	30	40
1 : 2	618nm	598nm	592nm	589nm
1 : 3	516nm	510nm	504nm	500nm
1 : 4	612nm	593nm	580nm	530nm

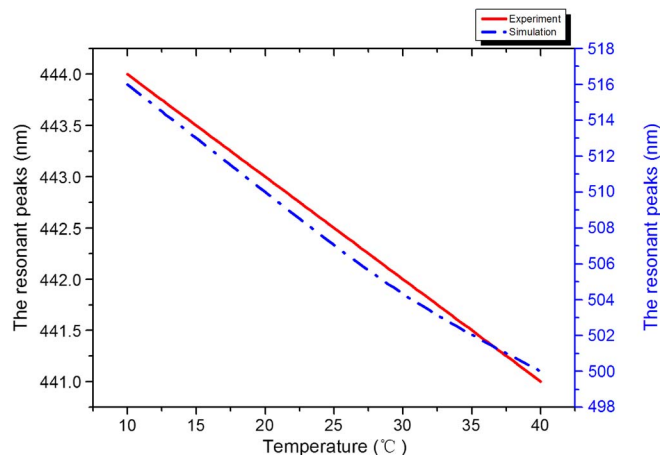


Fig. 7. Results of experiment and simulation as functions of temperature.

this experimental setup, a continuous spectrum fiber laser has been taken as the light source. The beam will be divided into two beams of light after being coupled into the single mode fiber (SMF) through the 3 dB coupler, and then both of them spread into two PCFs filled with and without analyte, respectively. The spectrograph is used to detect the change of resonance absorption peaks. Therefore, we can obtain information about the analyte according to the change of the resonance wavelength.

To measure the temperature dependence, we have realized the experiment of the temperature sensing with PCF filled with different concentrations at different temperatures. Fig. 6(a)–(c) present the change of the resonant peaks from 10 °C to 40 °C as a function of wavelength with at a certain proportion of the analyte, which shows the changes obviously. It's obvious to note that some sub-peaks will appear, which are some noise or other coupling effect. Ordinarily, the coupling can support several waveguide modes which result in several peaks, while only the most obvious resonant peak is the coupling between plasmonic mode and the core-guided mode, and others are the coupling between the core-guided mode and the higher order mode, generally. And we only consider the main resonant peak shift for sensing.

From the relationships between temperature and wavelength shift, the maximum temperature sensitivities can be obtained, which are 1 nm/°C, 0.6 nm/°C, 2.7 nm/°C, respectively corresponding to the different ratios of analyte of 1 : 2, 1 : 3, and 1 : 4. The experimental results indicate that a blue-shift will be obtained with the increase of the temperature, but the changing trends exhibit difference with different ratios of analyte. In general, the lower temperature, the higher sensitivity can be obtained. However, it shows a larger shift with the higher temperature when the ratio is 1 : 4, and the resonant shift is larger. The detailed information of the experiments showed is presented in Table 1.

The similar simulated and experimental results have been shown in Fig. 7, which show that the comparison of simulation and experiment exhibits a same trend with the change of temperature. When the temperature increases, a blue-shift will be obtained.

4. Conclusion

In this paper, we have analyzed a surface plasmon resonance temperature sensor based on LMA-8 PCF filled with nanowires and different concentrations of analyte in theory and experiment. The proposed sensor based on PCF has some advantages. First, PCF can be used as a channel either optical transmission or analyte, which can realize the interaction of light and matter. Second, the PCF has been produced by some researchers. Finally, the most important is that we have demonstrated the feasibility with a series of experiments. The results of simulation and the experiments show that the temperature influences the filled mixed liquid refractive indices leading to that the fundamental mode effective index is sensitive to the changes of the analyte RI, which can achieve temperature sensing. A blue shift will be obtained with the increase of the temperature, and the lower temperature shows a higher sensitivity generally. In the experiment, we can obtain the highest sensitivity of 2.7 nm/°C. The theoretical analysis and experimental results in this latter can provide reference for the implementation and application of PCF-based SPR temperature sensor or other PCF-based SPR sensing. Based on the above discussion and analysis results, we expect that the proposed PCF-based SPR temperature sensor can provide an effective platform for more sensing fields.

References

- [1] B. Eggleton, C. Kerbage, P. Westbrook, R. Windeler, and A. Hale, "Microstructured optical fiber devices," *Opt. Exp.*, vol. 9, no. 13, pp. 698–713, Dec. 2001.
- [2] R. T. Bise *et al.*, "Tunable photonic band gap fiber," in *Proc. Opt. Fiber Commun. Conf. Exhib.*, 2002, pp. 466–468.
- [3] L. Jing, J.-q. Yao, X.-h. Huang, and Y. Lu, "C₂H₂ sensing at $\nu_1 + \nu_3$ band with a hollow-core photonic bandgap fiber," *Optoelectron. Lett.*, vol. 7, no. 6, pp. 463–465, Nov. 2011.
- [4] B. Shuai, L. Xia, Y. Zhang, and D. Liu, "A multi-core holey fiber based plasmonic sensor with large detection range and high linearity," *Opt. Exp.*, vol. 20, no. 6, pp. 5974–5986, Mar. 2012.
- [5] T. Alkeskjold *et al.*, "All-optical modulation in dye-doped nematic liquid crystal photonic bandgap fibers," *Opt. Exp.*, vol. 12, no. 24, pp. 5857–5871, Nov. 2004.
- [6] W. B. Tanya *et al.*, "Sensing with microstructured optical fibres," *Meas. Sci. Technol.*, vol. 12, no. 7, pp. 854–858, Jul. 2001.
- [7] B. Lee, S. Roh, and J. Park, "Current status of micro- and nano-structured optical fiber sensors," *Opt. Fiber Technol.*, vol. 15, no. 3, pp. 209–221, Jun. 2009.
- [8] R. C. Jorgenson and S. S. Yee, "A fiber-optic chemical sensor based on surface plasmon resonance," *Sens. Actuators B, Chem.*, vol. 12, no. 3, pp. 213–220, Apr. 1993.
- [9] A. K. Sharma, R. Jha, and B. D. Gupta, "Fiber-optic sensors based on surface plasmon resonance: A comprehensive review," *IEEE Sensors J.*, vol. 7, no. 8, pp. 1118–1129, Aug. 2007.
- [10] C. Perrotton, N. Javahiraly, M. Slaman, B. Dam, and P. Meyrueis, "Fiber optic surface plasmon resonance sensor based on wavelength modulation for hydrogen sensing," *Opt. Exp.*, vol. 19, no. S6, pp. A1175–A1183, Nov. 2011.
- [11] Y. Zhang *et al.*, "Microstructured fiber based plasmonic index sensor with optimized accuracy and calibration relation in large dynamic range," *Opt. Commun.*, vol. 284, no. 18, pp. 4161–4166, Aug. 2011.
- [12] X. Yu *et al.*, "A selectively coated photonic crystal fiber based surface plasmon resonance sensor," *J. Opt.*, vol. 12, no. 1, p. 015005, Jan. 2010.
- [13] A. Hassani and M. Skorobogatiy, "Design criteria for microstructured-optical-fiber-based surface-plasmon-resonance sensors," *J. Opt. Soc. Amer. B*, vol. 24, no. 6, pp. 1423–1429, Jun. 2007.
- [14] X. Fu *et al.*, "Surface plasmon resonance sensor based on photonic crystal fiber filled with silver nanowires," *Opt. Appl.*, vol. 41, no. 4, pp. 941–951, Dec. 2011.
- [15] C. Zhou, Y. Zhang, L. Xia, and D. Liu, "Photonic crystal fiber sensor based on hybrid mechanisms: Plasmonic and directional resonance crystal coupling," *Opt. Commun.*, vol. 285, no. 9, pp. 2466–2471, May 2012.
- [16] T. Larsen, A. Bjarklev, D. Hermann, and J. Broeng, "Optical devices based on liquid crystal photonic bandgap fibres," *Opt. Exp.*, vol. 11, no. 20, pp. 2589–2596, Oct. 2003.
- [17] F. Du, Y.-Q. Lu, and S.-T. Wu, "Electrically tunable liquid-crystal photonic crystal fiber," *Appl. Phys. Lett.*, vol. 85, no. 12, pp. 2181–2183, Sep. 2004.
- [18] Y. Yu *et al.*, "Some features of the photonic crystal fiber temperature sensor with liquid ethanol filling," *Opt. Exp.*, vol. 18, no. 15, pp. 15 383–15 388, Jul. 2010.
- [19] Y. Peng, J. Hou, Z. Huang, and Q. Lu, "Temperature sensor based on surface plasmon resonance within selectively coated photonic crystal fiber," *Appl. Opt.*, vol. 51, no. 26, pp. 6361–6367, Sep. 2012.
- [20] Y. Peng *et al.*, "Temperature sensing using the bandgap-like effect in a selectively liquid-filled photonic crystal fiber," *Opt. Lett.*, vol. 38, no. 3, pp. 263–265, Feb. 2013.
- [21] B. Gauvreau, A. Hassani, M. Fassi Fehri, A. Kabashin, and M. A. Skorobogatiy, "Photonic bandgap fiber-based surface plasmon resonance sensors," *Opt. Exp.*, vol. 15, no. 18, pp. 11 413–11 426, Sep. 2007.